



## AN OBSERVATIONAL AND NUMERICAL STUDY OF A SEVERE AIR POLLUTION OVER TEHRAN MEGACITY

Sara Karami<sup>1\*</sup>, Abbas Ranjbar<sup>1</sup>, Amirhossein Nikfal<sup>1</sup>, Faezeh Noori<sup>1</sup>, Saviz Sehatkashani<sup>1</sup>

<sup>1</sup> Atmospheric Science and Meteorological Research Center (ASMERC), Tehran, Iran

### ARTICLE INFORMATION

#### Article Chronology:

Received 7 January 2018

Revised 5 February 2018

Accepted 10 March 2018

Published 29 March 2018

#### Keywords:

Air pollution; WRF model; YUS scheme; boundary layer; LASAT Model.

### CORRESPONDING AUTHOR:

Karamis.62@gmail.com  
Tel: (+9821) 44787651-5  
Fax: (+9821) 44787670

### ABSTRACT:

**Introduction:** Nowadays, air pollution is one of the most important problems, leading to serious financial and human health concerns. On the 15<sup>th</sup> to 17<sup>th</sup> days of November, 2016 an intense air pollution episode occurred in Tehran, Iran.

**Materials and methods:** In this study, the meteorological data, pollutant concentration, and the data related to this severe air pollution episode, required to implement the model, besides, a brief account, pertinent to the configuration of atmospheric model WRF and air quality model LASAT is presented and certain meteorological quantity are studied.

**Results:** Statistical analysis indicates in this case study, negative wind speed anomaly and positive mean temperature anomaly related to the average 65 years for Novembers. The minimum visibility, is reported for the two days of November 15 and 16. Atmospheric vertical structure analysis shows the temperature inversion at 950 hPa height on November 14<sup>th</sup>, 2016, it causes stable atmospheric conditions.

**Conclusions:** Running WRF model, with YSU boundary layer scheme, shows that it can well simulate the atmospheric quantities, however, the 10 m wind speed has more errors among the quantities. In this case study LASAT Model is applied for simulation of different pollutant concentrations. The results indicate the underestimation of model by using the output of WRF as atmospheric model is not dependent on the meteorological data, whereas the reference error is driven either from the parameterization, or from the estimation of pollutants emission related to ground level.

### INTRODUCTION

The effects of climate and meteorological factors on urban problems such as air pollution, heat island, and urban hydrology have increasingly become important in terms of mitigation and adaptation issues during the recent years [1]. Aero-

sol particles impact the planet's energy balance, the hydrologic cycle, atmospheric visibility, and public health. The relative strength of particles in imparting these effects depends largely on their abundance and physicochemical properties, which are governed by emission sources, trans-

port, and meteorology. Reduction of air quality creates several problems for communities' health condition, particularly for a vulnerable population, including elderly and children [2 - 5] to such an extent that the number of patients who refer to the health care centers, especially with heart and respiratory diseases, dramatically increase [6 -10]. Furthermore, regarding previous studies, a relation between mortality rate and air pollution has been reviewed [11, 12]. Moreover, studies have been done on the effect of atmospheric quality on the air pollution, which include upper air meteorological condition of acute air pollution episodes [13]; relationship between synoptic scale atmospheric circulation and ozone concentration [14]; coastal and synoptic recirculation affecting air pollutants dispersion [15]; synoptic and mesoscale weather conditions during air pollution episodes in Athens, Greece [16]. In Tehran city, air quality reduction as a devastating problem, occurs in autumn and winter seasons [17]; in this connection, having considered certain cases, pollutants concentration increases, to such an extent, leading to closure of schools and offices. Moreover, on the days 15 through 17 of November 2016, Tehran city's air pollution was severely high, led to closure of all the elementary schools; however, additional traffic banned areas as a solution implemented to, the pollution persistently continued for more days, consequently caused the critical condition. One of the effective elements on reducing the air quality is the atmospheric conditions prevailing over a region; hence, in this study, aimed to define air pollution conditions prevailing atmospheric patterns effective on early warning and reduction of likely damages. By timely prediction and warning notices damages, to certain extent, can be reduced, due to air pollution increase, many numerical models including AERMOD [18]; CALPUFF

[19], HYSPLIT [20] and ADMS [21], have been developed for air pollution prediction, across the world. LASAT model (Lagrangian Simulation of Aerosol Transport) [22] which has been implemented for Tehran city, is being assessed in this study.

In this study, the meteorological data, pollutant concentration, and the data, required to implement the model, besides that a brief account, pertinent to the configuration of atmospheric model WRF and air quality model LASAT is presented and certain meteorological quantity are studied, taken from 3 stations, located in the north, south and west of Tehran. Then, the synoptic condition, prevailing the area is exhibited and certain quantities, relevant to the atmospheric boundary layer, including its height out of WRF model are studied. The temperature and wind speed, dependent on WRF are evaluated. Finally, the data of the different pollutant concentrations are studied and the output of LASAT model is compared to the observed data in this case study.

## MATERIALS AND METHODS

The center of Tehran city is on latitude  $35^{\circ}41'$  N and longitude  $51^{\circ}26'$  E. Tehran is located in the steep southern slopes of the Alborz mountain range, which traces an arc along the coast of Caspian Sea in northern Iran. Its highest peak, mount Damavand, has an elevation of more than 5,600 m and is visible from Tehran in clear days (<https://www.britannica.com/place/Tehran>).

Tehran features a cold semi-arid climate with continental climate characteristics and a mediterranean climate precipitation pattern. Tehran's climate is largely defined by its geographic location, with the towering Alborz mountains to its north and the country's central desert to the south. It can be generally described as mild in spring and autumn, hot and dry in summer, and cold and wet

in winter. Because the city is large with significant differences in elevation among various districts, the weather is often cooler in the hilly north than in the flat southern part of Tehran.

The northernmost limits of the city stand at about 1,700 m above sea level and the southernmost limits about 1,100 m. There is a difference of about 600 m between the northern heights and the southern edges of the city, some 30 km away. This dramatic difference in height and Tehran's location between mountains and desert have had significant impacts on the social and physical characteristics of the city. Alborz Mountains surrounded north and northeast of Tehran like a dam, which act against western winds and causes to remain all pollution on the city surface. Tehran is affected by Alborz Mountains, different inversions and continental high pressure systems, so Tehran air pollution cannot be reduced or removed by natural conditions of area [23]. Tehran's topography as well as geographic locations of the ground - based air pollution monitoring stations is depicted in the Fig. 1.

In this study, the data of temperature, mean sea level pressure, visibility and wind speed are studied, relying on the synoptic meteorology stations,

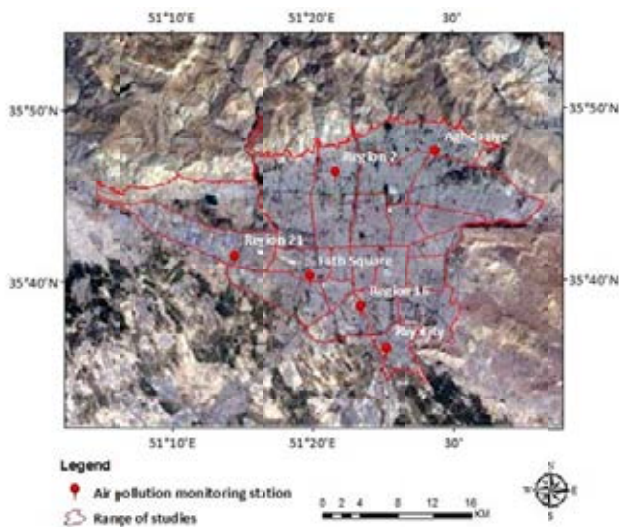


Fig. 1. Geographic locations of the ground - based air pollution monitoring stations

of Shemiran, Imam Khomeini and Mehrabad airports, respectively located in the north, south and west of Tehran on the days of 14 to 17 of November 2016. In order to understand the magnitude of prevailing patterns, synoptic analysis is presented by means of mean sea level pressure and geopotential height at 500 hPa level plots, driven from WRF model output. At the beginning, the observed data of mean sea level pressure, the 2 m. Temperature and the 10 m wind, obtained from Tehran's Mehrabad airport station are compared to the model's output; then, certain quantities, pertinent to the boundary layer, for instance the height of boundary layer,  $u^*$ ,  $w^*$ , and the height of entrainment layer are combined, besides that the bulk Richardson number and the structure of vertical temperature and wind, driven from the Model output, are presented.

Tehran air pollution levels are investigated by considering the maximum daily concentrations of CO and NO<sub>2</sub>, and the average daily concentrations of PM<sub>10</sub>, PM<sub>2.5</sub> and SO<sub>2</sub>. Furthermore, the air quality indices for five classifications (good, moderate, unhealthy for sensitive groups, unhealthy, and hazardous) are taken into account for Tehran urban area. For considering the changes in pollution levels, time series of the mean hourly values of PM<sub>10</sub>, PM<sub>2.5</sub>, CO, and NO<sub>2</sub> which exceed the standard values, are depicted. Consequently, the outputs of LASAT air quality model for PM<sub>10</sub>, CO, and NO<sub>2</sub> concentrations over north, south, and west of Tehran are compared with the observational data, and the possible sources of model errors are discussed.

The meteorological data, used are the quantities containing temperature, wind, pressure, and visibility, related to the three synoptic stations of Shemiran, Mehrabad and Imam-Khomeini air ports in the existing 3 h period, taken from the Iran Meteorological Organization. For PM<sub>10</sub>, the charac-

teristics of these synoptic stations are displayed whereas, Shemiran has the highest altitude and Imam - Khomeini air port has the lowest altitude, above the mean sea level.

The GFS data, with 0.5degree resolution (<ftp://nomads.ncdc.noaa.gov/GFS/Grid4/>) are used for initial and boundary conditions of WRF Model. The different pollutant concentrations, in the mean hour and day, at some stations, located in the N, S, and W of Tehran released by Tehran Air Quality Control Company, are displayed in the Fig. 1.

At first, for synoptic analysis, the model WRF is run on a grid with a horizontal spacing of 30 km, 100 points along west - east, and 105 points along south - north (Fig. 2). The schemes employed in the running processes are listed in Table 2.

For analyzing atmospheric conditions over the study period on 14 – 17 November 2016, the WRF model is run with 3 nested domains by horizontal resolutions of 27, 9, and 3 km and 40 vertical levels (Fig. 2).

The schemes, used for the second run, is similar to the previous one. The boundary layer scheme

has an important role in calculating the air pollution level. A study, modeled the boundary layer over three months of summer, by means of three different boundary layer schemes, including MYJ (Mellor – Yamada – Janjic), YSU (Yonsei University), and ACM2 (Asymmetric Convective Model version 2), with the WRF model, and compared the surface observations with the modeled boundary layer in parts of Texas, the United States [27]. Due to disregarding of the entrainment processes at the top of boundary layer, the performance of MYJ scheme shows more errors in modeling of the boundary layer, compared with YSU and ASM2 schemes; Therefore, the YSU boundary layer scheme is employed in the current study. The YSU scheme [28], [26], is a new version of K-Theory, considering the role of large scale eddies in the total atmospheric flux. In this scheme the turbulent diffusion equation for the prognostic quantity of C (for instance, temperature, wind speed components, etc.) is expressed as follow:

$$\frac{\partial c}{\partial t} = \frac{\partial}{\partial z} \left\{ K_c \left( \frac{\partial c}{\partial z} - \gamma_c \right) - \overline{(w'c)'}_h \left( \frac{z}{h} \right)^3 \right\} \quad (1)$$

Table 1. The characteristics of the synoptic stations

Station	ID	Lat.	Lon.	Height	Geographical location in Tehran
Shemiran	40751	35.799	51.48	1549.1	North
Mehrabad airport	40754	35.693	51.312	1191	West
Imam Khomeini airport	40777	35.42	51.17	990.2	South

Table 2. WRF model schemes

Microphysics	WRF Single - Moment 5- class scheme
Long wave radiation	RRTM scheme [24]
Short wave radiation	Goddard shortwave [25]
Surface physics	Noah Land Surface Model
Planetary boundary layer	Yonsei University scheme [26]
Cumulus	Grell 3D

Where,  $K$  is eddy diffusive coefficient, and  $\delta z$  is local gradient correction in which the role of large scale eddies is considered,  $h$  is the boundary layer thickness, defined as a level in which the minimum flux exists in the inversion layer. In this Eq.  $F$  is the flux inside the entrainment layer.

In YSU boundary layer scheme  $u^*$  is the velocity scale of mixed layer, obtained by means of friction velocity. Convection velocity scale is based on the Eq. (2), and somehow shows the vertical motion in the atmospheric boundary layer. The quantity  $w^*$  is equal to zero at night once the mixed layer is removed.

$$w^* = \left( u^{*3} + \frac{8kw_b^* z}{h} \right)^{1/3} \quad (2)$$

In the Eq. (2),  $u^*$  is friction velocity,  $w_b^*$  is the convection velocity scale,  $z$  is height above sea level and  $h$  is boundary layer height.

$$w_b^* = \left\{ \frac{g}{\theta} (\overline{w'\theta'})_0 h \right\}^{1/3} \quad (3)$$

Model LASAT is a Lagrangian Model, which

calculates dispersion and transfer of tracer particles in the atmosphere [22]. This model requires meteorological data as an input data to calculate gaseous dispersion over the urban areas. The meteorological input data for the model LASAT is provided by WRF model, afterwards is down-scaled by a diagnostic mesoscale model, named PROWIMO. In this paper, the LASAT model is configured for Tehran urban area with a horizontal grid resolution of 1 km.

## RESULTS AND DISCUSSION

The mean temperature of Mehrabad station in the month of November from 1951 through 2014 for 65 years is shown in the Fig. 3. The temperature values change from about 6 ° C to 16 in this period, and its average is equal to 11.6 ° C. Taking into consideration, the mean temperature of Mehrabad air port station is equal to 16.10 ° C on the days of 14 through 18 November 2016, which is almost 5 ° C more than the mean 65 years, it can be concluded, in a way, that the air temperature of this station has noticeably positive anomaly.

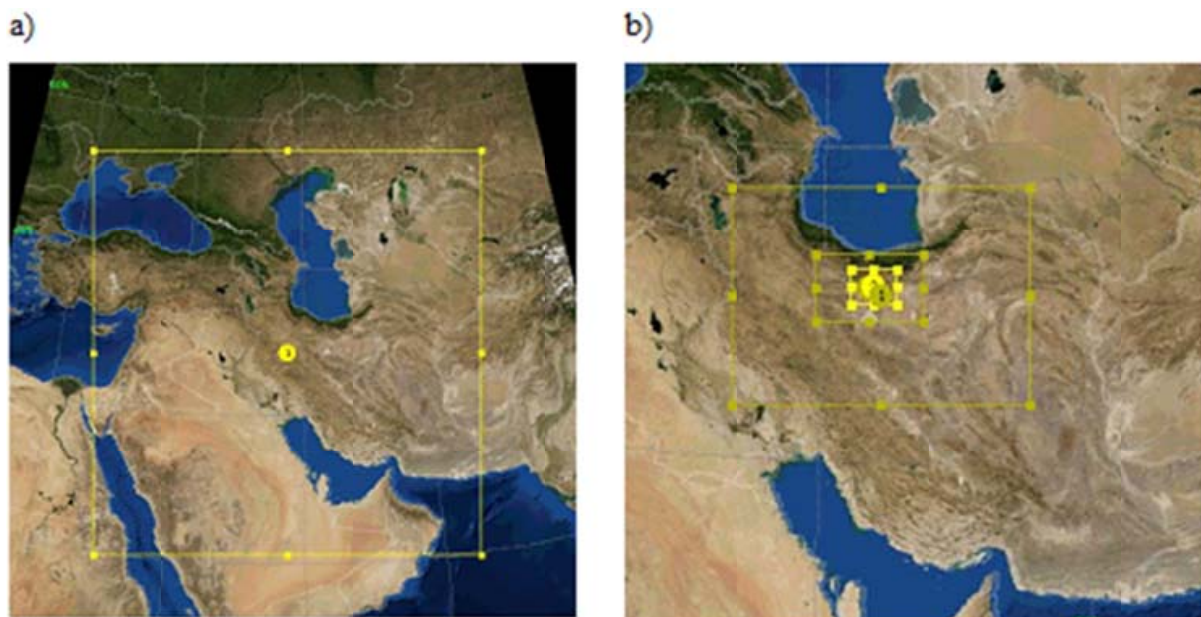


Fig. 2. Model domains in a) first run, b) second run with 3 nests

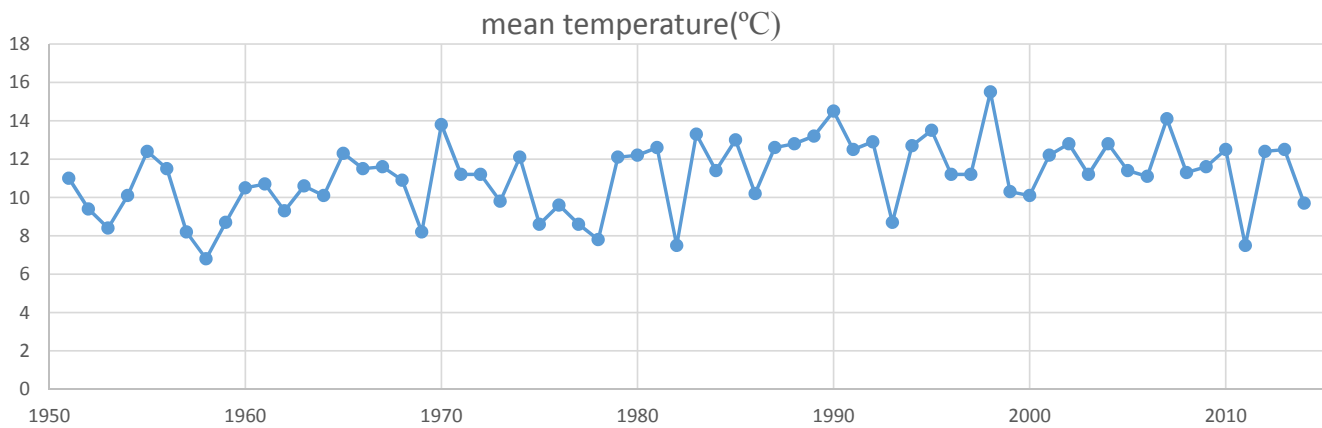


Fig. 3. The mean temperature of Mehrabad airport station in the month of November from 1951 through 2014 for 65 years

The mean wind speed of Mehrabad airport station is equal to 2 m / s during 65 years period, but in this case study the mean wind speed is 1.47 m / s which is less, relative to the mean value. In general, the negative anomaly of wind speed can be deemed as a factor, leading to the increase of Tehran's air pollution, under this case study. On the other hand, the increase of pollutants rate has a positive feedback for the temperature increase, which is effective in these few days, relative to the wind speed.

The graph of mean sea level pressure, provided by the three stations of Shermiran, Mehrabad and Imam - Khomeini airports for the days of 14 through 18 November in 2016 (Fig. 5.a), show the most atmospheric pressure which gradually begin to make the trend of pollutant concentration increase, covering Tehran city with air pollution, due to which, consequently it leads to closure of schools on the 15<sup>th</sup> of November. The pressure rate gradually decreases on the day of 15, leading to min. value on the 16<sup>th</sup> of November and

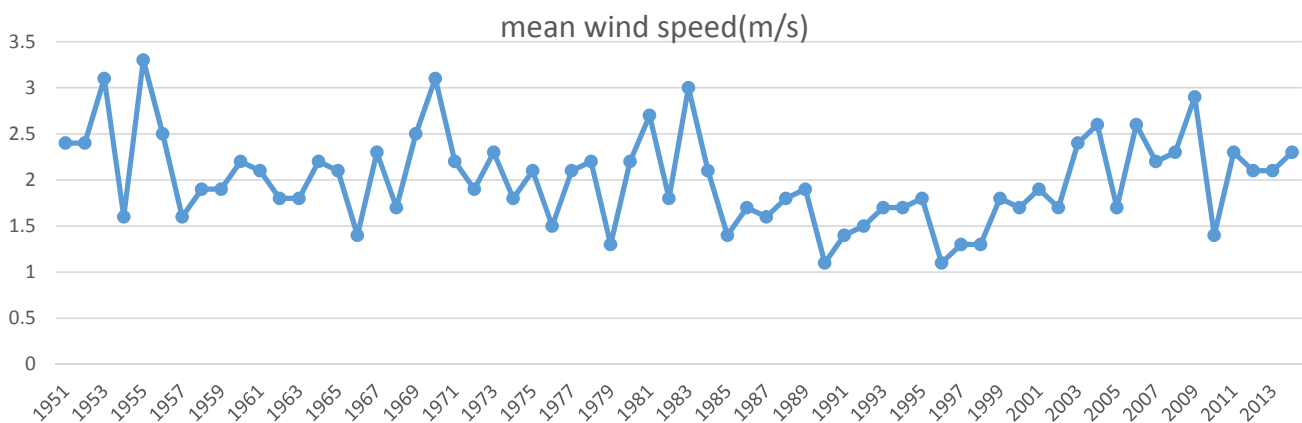


Fig. 4. The mean wind speed of Mehrabad airport station in the month of November from 1951 through 2014 for 65 years

again the little increase of pressure is seen in the three areas. The most sea level pressure value is reported, equal to 1022.7hPa for Imam Khomeini Air Port station, at 06 UTC on the day 14 Nov. and the min. value is registered equal to 1012.1 hPa at Mehrabad Station, at 12 UTC on the day of 16<sup>th</sup> of Nov.

According to the Fig. 5.b, it shows that the maximum temperature of each three stations, depends on the 14<sup>th</sup> day of Nov, then the maximum temperature drops versus the minimum temperature effectively increasing, accordingly the rate of daily changes of the temperature decreases, which is due to increase of pollutants concentration in the atmosphere, this event is because of the pollutants exist during the day time which stop sunlight shortwaves reach the ground level, consequently at night they stop the surface long waves outflow, resulting in the increase of minimum temperature. The maximum temperature is equal to 24.2°C at Imam Khomeini airport at 12UTC on the 14<sup>th</sup> day of November, and the min temperature is equal to 7°C at the same airport at 03 UTC h on the 15<sup>th</sup> day of November.

In Fig. 5. c the minimum visibility is registered at equal to 3000 m at Mehrabad station on the two days of 15<sup>th</sup> and 16<sup>th</sup> of November; then on the 16<sup>th</sup> day of November. It is reported, the visibility is equal to 4000 m at Imam airport on the day of 16<sup>th</sup> November and at Shermiran station the visibility is equal to 6000 m.

The time series showed in Fig. 5. d exhibit, wind speed is noticeably dropped at the two stations of Imam Khomeini and Mehrabad airports on the days of 15<sup>th</sup> and 16<sup>th</sup>, too. Also, the changes, in the wind speed, at Shemiran station, comparing to the other two stations are less.

The Skew -T diagram, pertinent to the days of 14<sup>th</sup> and 15<sup>th</sup> of November, 2016 (at 12 UTC) is displayed in the Fig. 6. On the 14<sup>th</sup> day of Nov.

the temperature inversion is observed at level 950 hPa, causing atmospheric stability and therefore, it stops pollutants to transfer to the upper levels of atmosphere, due to which the pollutants concentration is increased close to the surface. The wind speed in the lower levels is considerably reduced on the day 15<sup>th</sup> of November compared to the 14<sup>th</sup>, which itself caused pollutants remain in the atmosphere. The height of 850 hPa pressure level on the 15<sup>th</sup> of November compared to the previous day is little dropped, showing that the pressure is reduced at the lower levels. The positive lifted index value (LI) and the other index values show that the atmosphere is stable in each two days, however the stability rate is more in the 14<sup>th</sup> of November.

On 14<sup>th</sup> of November at 00UTC a high pressure system enters Iran from Turkey and affects many parts of the country, while another high pressure center is prevailed in Saudi Arabia, its ridges reach the southern areas of Iran. In the meantime, there is a weak low pressure center in the north of Caspian Sea, affecting the southern coasts of Caspian Sea. A high pressure center is formed over Tehran province, causing pressure increase in this area, relative to the surrounding areas. The 10 m wind speed in all the central regions of Iran is considerably lower than the other parts, so any prevailing direction cannot be deemed for it. The geopotential height plot at level 500 hPa shows a high center is prevailed in Saudi - Arabia its ridges dominating over Iran.

In order to evaluate the capability of the WRF model for the simulation of atmospheric variables, effective in air pollution, the quantities of mean sea level pressure, 2 m temperature and the observed wind speed at 10 m height are compared to the model output, with coordinates 35. 69 and 51, 31 E at Tehran's Mehrabad airport station. The modeled sea level pressure is in agreement



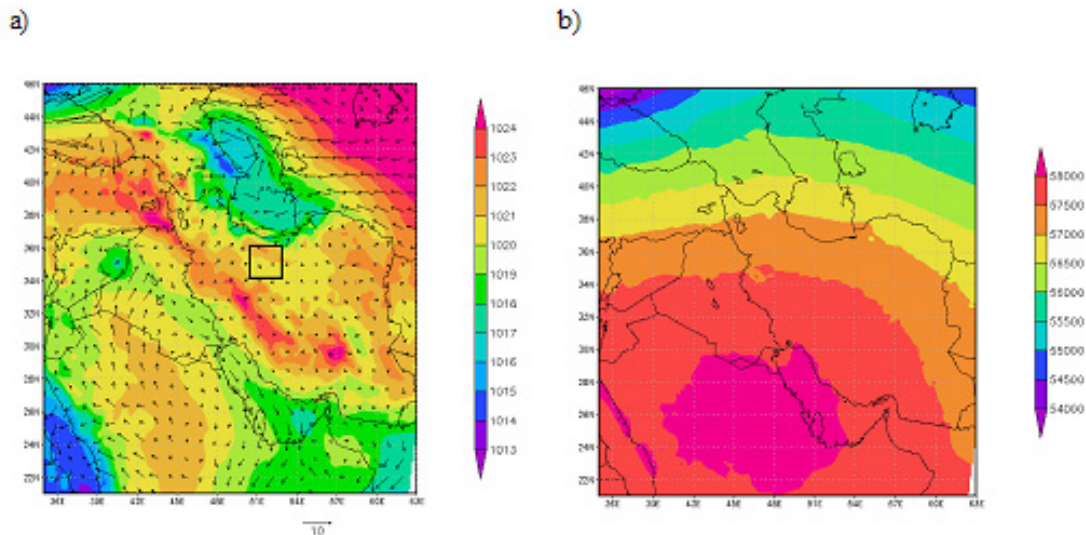


Fig. 7. a) Mean sea level pressure (hPa) and wind speed (m / s) at 10 m height b) geopotential height at 500 hPa level (m) on 14 November, 2016 at 00UTC

with the observed values, but with a minor over-estimation. WRF model shows almost identical pattern between the modeled 2 m temperature and the observations, except for the minimum temperatures with small overestimations. The parameter of 10 m wind speed from WRF model output is more contradicting than the observed values, in comparison of the two quantities of temperature and pressure. The trend of

wind speed is almost similar, except for the end of the day 15<sup>th</sup> of November; but the model underestimates the maximum wind speed values, and overestimates the minimum values. Since the quantity of wind speed value is a determining factor on the accuracy of the air quality model, the error in estimation of this quantity by the atmospheric model can make many errors in predicting the pollutants concentration.

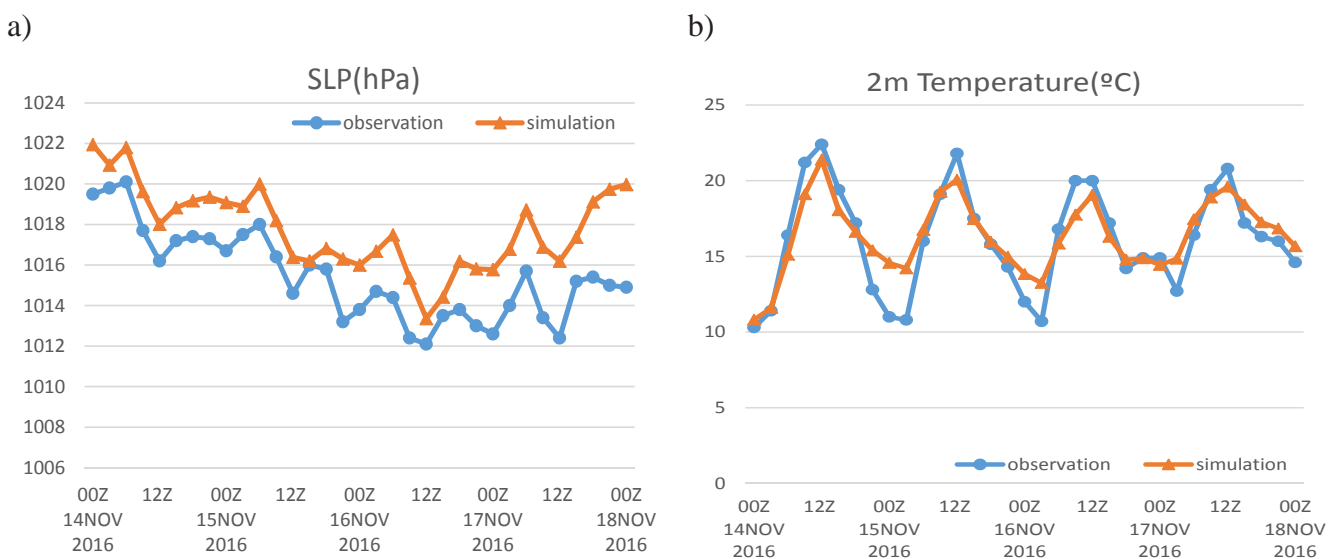


Fig. 8. a) Mean sea level pressure and b) 2m temperature from observation and WRF model output at Mehrabad airport station from 14 to 18 November 2016

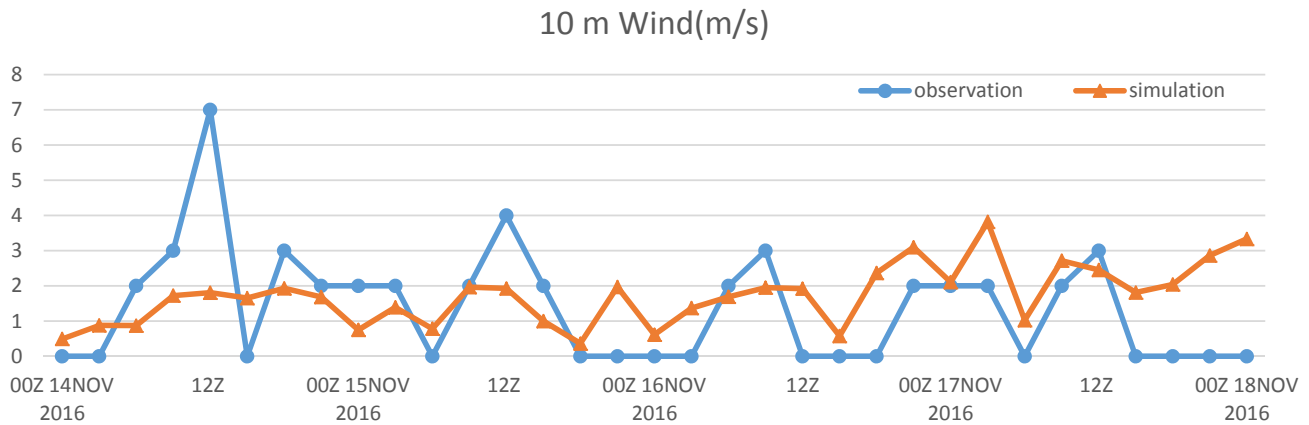


Fig. 9. The output of 10 m wind speed of WRF model and the observed values at Mehrabad station from November 14 to November 18, 2016

One of the quantities with direct impact on air pollution level is the atmospheric boundary layer (ABL) thickness that effects on pollution level in various methods such as transporting and dilution of air pollutants by wind and turbulent mixing inside the ABL. Therefore, the less the ABL thickness is, the more the air pollution level will be. Diurnal and nocturnal variations in ABL thickness are well simulated in the WRF model (Fig. 10) and the maximum and minimum ABL thickness occurs during the days and nights, respectively. The lowest value of the maximum ABL thickness over the study period occurs on the 15<sup>th</sup> of November with a height of 650 m. During the next days, towards the 17<sup>th</sup> of November, the maximum thickness of ABL increases to 1600 m. These variations of the ABL thickness are negatively correlated with the levels of air pollution on 14 and 15 November.

The values of friction velocity show the vertical shear of horizontal wind which has small values until the midday of 16<sup>th</sup> of November. The results show the values of mechanical dispersion, associated with the wind shear on the two days of 14 and 15 November, have the lowest values, but

gradually from the 16<sup>th</sup> of Nov, as the friction velocity increases, the level of air pollution drops. The low values of vertical speed ( $w^*$ ) in the mixed layer on 14<sup>th</sup> and 15<sup>th</sup> of November, is a determining factor in the rise of air pollution level. Gradually from 17<sup>th</sup> November,  $w^*$  shows a considerable increase and therefore, relative improvement of the air quality.

In YSU scheme, the effect of entrainment flux over the boundary layer is considered. Delta is a quantity which shows the depth of the entrainment layer in meter, obtained from YSU scheme which is about 17 m on 14<sup>th</sup> and 15<sup>th</sup> of November, and reaches to about 34 m on 17<sup>th</sup> of November. Decrease in the height of the entrainment layer reduces the effects of large scale eddies, flowing from the free atmosphere into the boundary layer, and rises the air pollution concentrations.

Richardson number is the ratio of the two terms of buoyancy and mechanical production in the equation of turbulent kinetic energy. Negative values of Richardson number account for atmospheric instability. For Richardson numbers less than the critical value of 0.25, mechanical instability is supposed to override static instability.

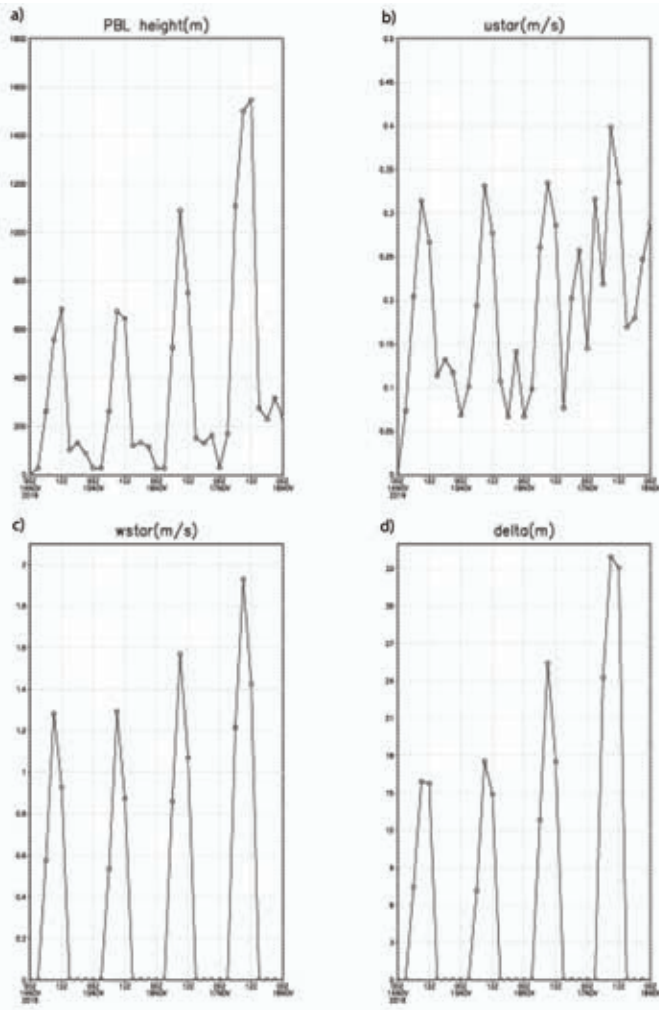


Fig. 10. a) Planetary boundary layer height, b) , c) , and d) entrainment layer depth from WRF model output at Mehrabad station from 14<sup>th</sup> to 18<sup>th</sup> of November, 2016

For the values greater than 0.25, static stability is the prevailing condition for the atmosphere. Bulk Richardson number is calculated, based on Eq. (4).

$$R_B = \frac{(g/T_v)\Delta\theta_v\Delta z}{(\Delta U)^2 + (\Delta V)^2} \quad (4)$$

Fig. 11 shows that over the 4 days of WRF model simulation, the bulk Richardson number has small negative values between hours 06 and 12 UTC, indicating weak static instability. For the other values showing positive Richardson numbers, especially for the values greater than 0.25,

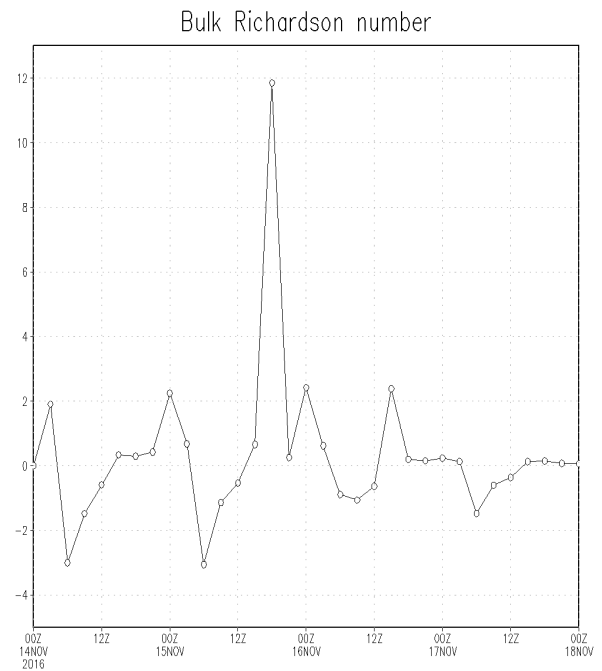


Fig. 11. Bulk Richardson number from WRF model output at Mehrabad airport station from 14<sup>th</sup> to 18<sup>th</sup> of November, 2016

the atmospheric conditions are modeled as statically stable.

Vertical profile of temperature (Fig. 12 - a), on 14<sup>th</sup> of November, 00 UTC, shows a relatively intense instability in the low levels of atmosphere. Moreover, the wind profile (Fig. 12-b) shows a small drop in the surface wind speed with respect to height ground level. As a whole, the vertical profile of temperature and the wind, simulated by the model are very consistent to the Skew-T diagram. In this study, the concentrations of several criteria pollutants, such as CO, NO<sub>2</sub>, PM<sub>10</sub>, PM<sub>2.5</sub>, and SO<sub>2</sub> are classified with regard to the values of the standard air quality index and presented in Table 3. Since, none of the stations data over the study period were complete, data from the neighboring stations are employed to compensate for the missing values. The concentrations of PM<sub>10</sub> and SO<sub>2</sub> are in the clean and healthy condition in all the areas over the study period. Considering the

air quality index, the levels of  $PM_{10}$ ,  $SO_2$ , and CO are classified as healthy conditions, whereas for the levels of  $NO_2$  and  $PM_{2.5}$ , the air quality is classified as unhealthy and very unhealthy over the 4 days of study period. The maximum mean daily value of  $PM_{2.5}$  is occurred in south of Tehran on 17<sup>th</sup> of November, while for the west and north of Tehran, this value is reported on 14<sup>th</sup> and 15<sup>th</sup> of November, respectively.

Times series of  $PM_{10}$  concentrations (Fig. 13) shows that its values in western Tehran are considerably higher than in the north and south of Tehran. This condition can be explained by the presence of agricultural lands and arid regions which act as dust sources in west parts of Tehran, where as a result of the heavier weight, the main part of them is settled in the same western areas of the city.

The pollutant  $NO_2$  is more produced, due to the

traffics on the roads. In this study, The  $NO_2$  concentrations in the north of Tehran are considerably lower than the south and west of the city. The highest monitored concentration value is equal to 226 ppb in south of Tehran on 15<sup>th</sup> of November 2016 at 10 UTC. The CO concentration on 16<sup>th</sup> and 17<sup>th</sup> of November is higher in the west of Tehran, compared to the north and south of the city.

For the evaluation of LASAT model, the concentrations of CO,  $PM_{10}$  and  $NO_2$  are displayed at 3 stations, located in north, south, and west of Tehran. Although the model shows an acceptable performance in simulating the time series of air pollution concentrations, there are considerable differences between the modeled and the observed values of pollutants. The LASAT model well simulates the time series of  $PM_{10}$  concentration at each 3 areas. For the gaseous pollutants,

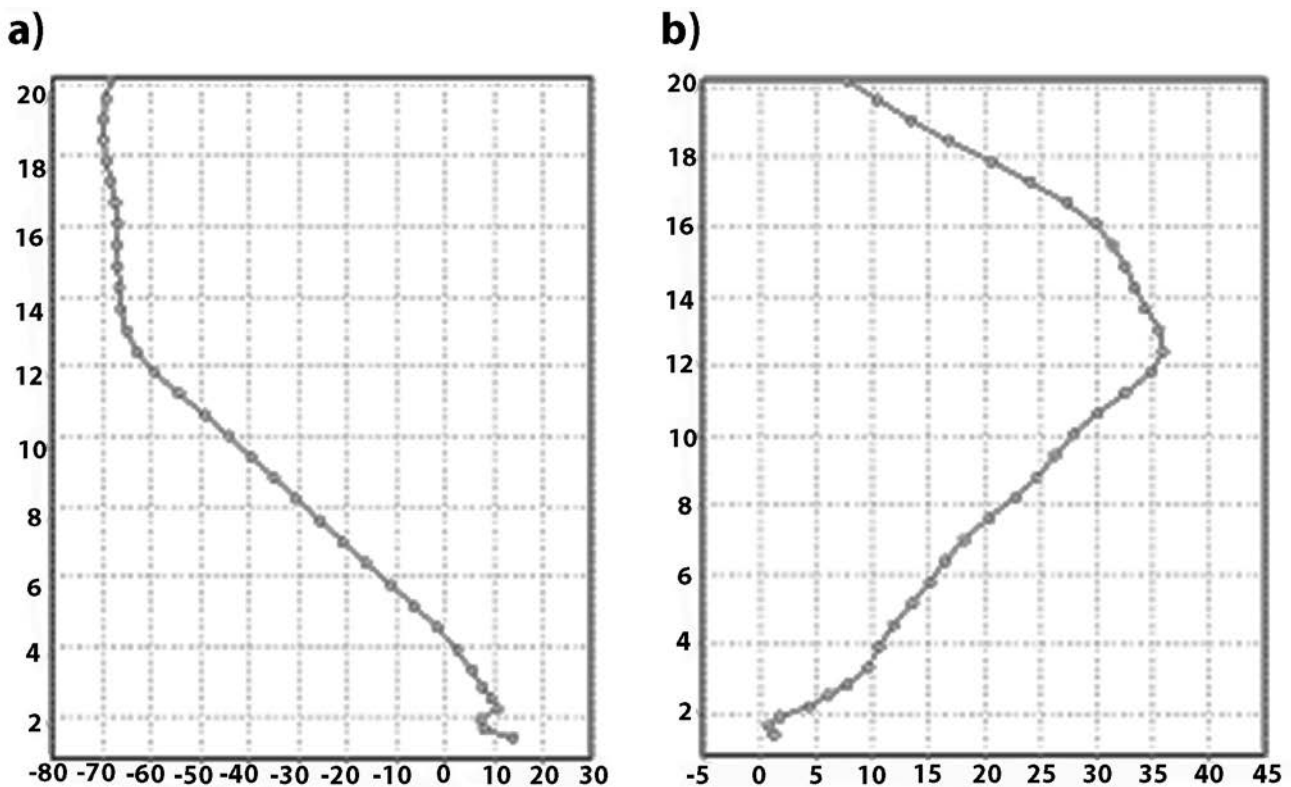


Fig. 12. The vertical structure of a) temperature ( $^{\circ}C$ ), b) wind speed (m / s) at Mehrabad station on 14<sup>th</sup> of November, 2016 at 00UTC

Table 3. The maximum hourly values of CO and NO<sub>2</sub> and the daily mean concentration of PM<sub>10</sub>, PM<sub>2.5</sub> and SO<sub>2</sub> in the north, south and west of Tehran on 14<sup>th</sup> - 17<sup>th</sup> of November, 2016

Concentration	11/14/2016	11/15/2016	11/16/2016	11/17/2016
CO_W (PPM) Max (1 h)	11.7	11.3	14.4	15.6
CO_N (PPM) Max (1 h)	4.5	4	5.6	4.4
CO_S (PPM) Max (1 h)	9.1	7.3	6.5	5.7
NO <sub>2</sub> _W (ppb) Max (1h)	175	208	147	178
NO <sub>2</sub> _N (ppb) Max (1 h)	109	138	123	100
NO <sub>2</sub> _S (ppb) Max (1 h)	180	226	173	153
SO <sub>2</sub> _W(ppb) Mean (24 h )	28	41	40	48
SO <sub>2</sub> _N (ppb) Mean (24 h)	33	44	40	41
SO <sub>2</sub> _S (ppb) Mean (24 h)	20	47	45	19
PM <sub>10</sub> _W(μg / m <sup>3</sup> ) Mean (24 h)	136	139	126	153
PM <sub>10</sub> _N(μg / m <sup>3</sup> ) Mean (24h )	102	96	87	91
PM <sub>10</sub> _S (μg / m <sup>3</sup> ) Mean (24h)	113	138	115	150
PM <sub>2.5</sub> _W(μg / m <sup>3</sup> ) Mean(24h )	161	169	153	168
PM <sub>2.5</sub> _N(μg / m <sup>3</sup> ) Mean (24h)	182	167	105	115
PM <sub>2.5</sub> _S (μg / m <sup>3</sup> ) Mean (24 h )	199	199	201	210

time series of NO<sub>2</sub> concentration show better agreement with the observations, compared to CO in the west of Tehran, furthermore in the south and north of Tehran, time series of CO concentrations is in better agreement with the observations,

rather than NO<sub>2</sub>. LASAT model uses the output of WRF modeling system as a driver for gaseous dispersion calculations. Since the WRF model has a reliable performance in the simulation of meteorological parameters, the noticeable errors

in LASAT outputs correspond to emissions. Various air quality monitoring stations are located in street canyons. It must be considered that street canyons cannot be imaged by the LASAT model which calculates for a grid cell of  $1 \text{ km} \times 1 \text{ km}$  in Tehran. Air pollution concentrations in street canyons are higher than behind buildings. This issue besides the low accuracy of emission data are the main reasons for the high errors in the

LASAT model results. For rectifying such errors, the implementation of special microscale air flow can lead to more reliable results.

## CONCLUSIONS

According to the report of the air quality control organization, on 15<sup>th</sup> - 17<sup>th</sup> of November, 2016, the air pollution in Tehran city reached to a severe level and caused health warnings of emergency

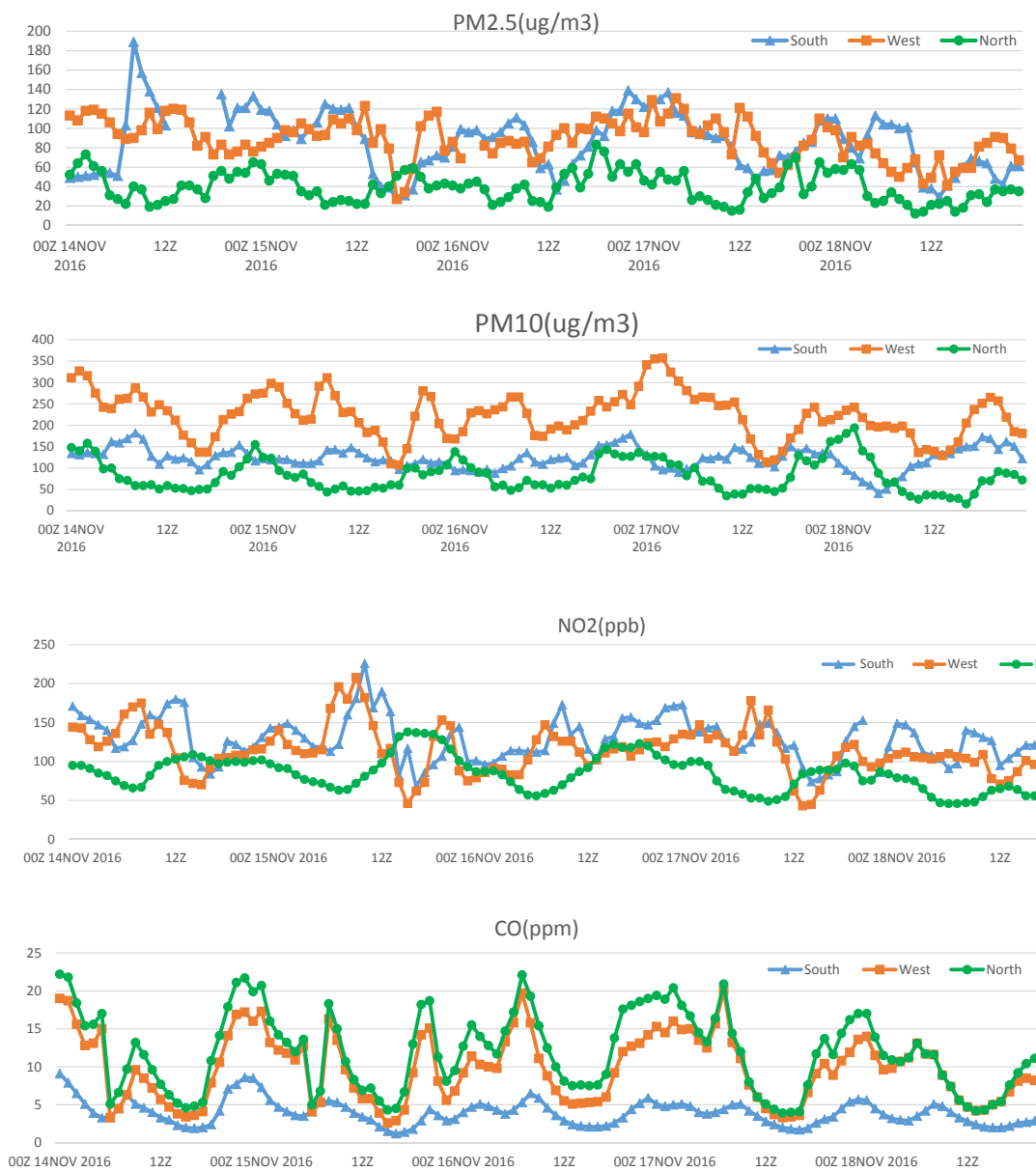


Fig. 13. The hourly concentration of a)  $\text{PM}_{2.5}$  ( $\mu\text{g} / \text{m}^3$ ); b)  $\text{PM}_{10}$  ( $\mu\text{g} / \text{m}^3$ ); c)  $\text{NO}_2$  (ppb); d) CO (ppm) in the north, south and west of Tehran on 14<sup>th</sup> - 19<sup>th</sup> of November, 2016

conditions. Generally, the temperature inversion, stable atmosphere, and great reduction in wind speed are considered as contributory factors in this air pollution episode. Furthermore, on 15<sup>th</sup> of November, the amounts of daily temperature and visibility show a drop, due to the increase in air pollution concentrations. This condition is more noticeable at the early hours of the day, when the boundary layer is at minimum height.

Evaluation of the results of the WRF model shows an acceptable agreement between modeled and observed values for the parameters of mean sea level pressure, 2 m temperature, and 10 m wind speed. However, there are some discrepancies between the modeled and the observed 2 m wind speed. Daily variations in the height of boundary layer are well shown by the WRF model results, corresponding its maximum and minimum heights to diurnal and nocturnal periodicity, respectively. On November 15, the boundary layer reaches its minimum height, which is consistent with the high pollution concentrations on November 14<sup>th</sup> and 15<sup>th</sup>. Overall, reductions in

friction velocity, vertical speed, and the height of entrainment layer and turbulent effects on 14<sup>th</sup> and 15<sup>th</sup> of November 2016 agree with the rise in concentrations of pollutants. Furthermore, the vertical profile of temperature and wind simulated by WRF model are very similar to the Skew-T diagram.

Regarding LASAT model, under case study, its performance shows the concentration pollutants, CO, PM<sub>10</sub>, and NO<sub>2</sub> at the 3 stations, located in the north, south, and west of Tehran. This model estimates most of the pollutants with a considerable underestimation in comparison to the observations. Many monitoring stations are located in street canyons which cannot be imaged by LASAT model in Tehran. Such effects can be calculated only with high horizontal resolution of the applied dispersion model. This issue besides the low accuracy of emission data are the main reasons for the high errors in the LASAT model results. For rectifying such errors, the implementation of special microscale air flow can be led to more reliable results.

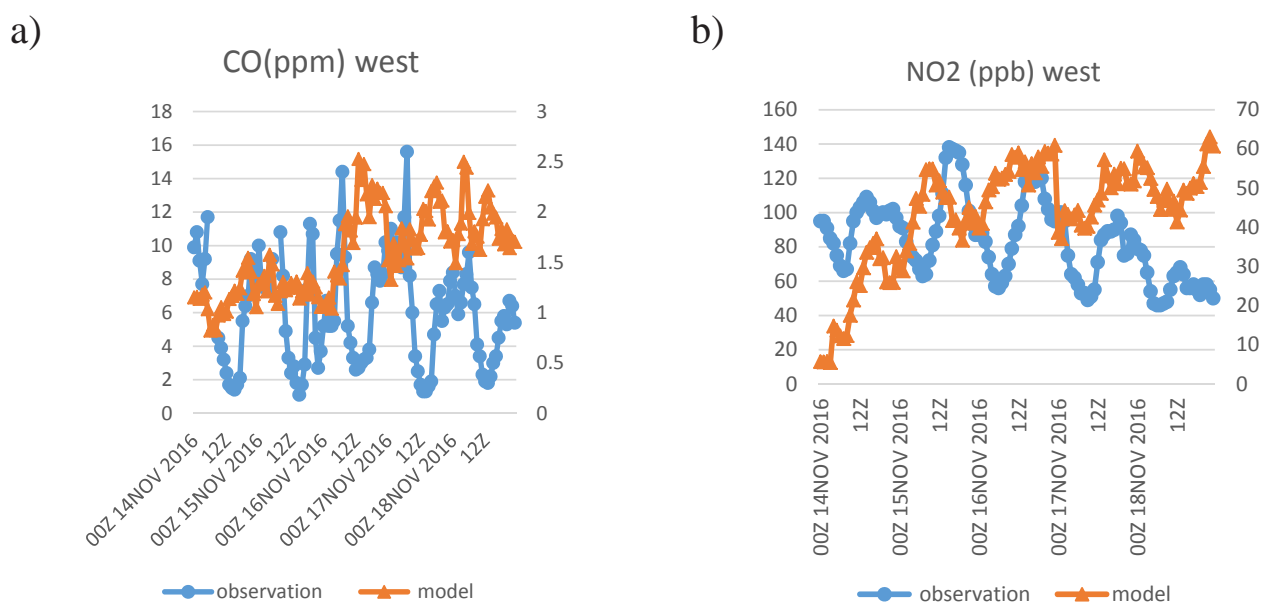


Fig. 14. a, b, and c) Simulated (red diagram, left vertical axis) and observed (blue diagram, right vertical axis) concentrations of CO, NO<sub>2</sub>, and PM<sub>10</sub>, respectively, for the west of Tehran. d, e, and f) same as a, b, and c, for the south of Tehran. g, h, and i) same as a, b, and c, for the north of Tehran

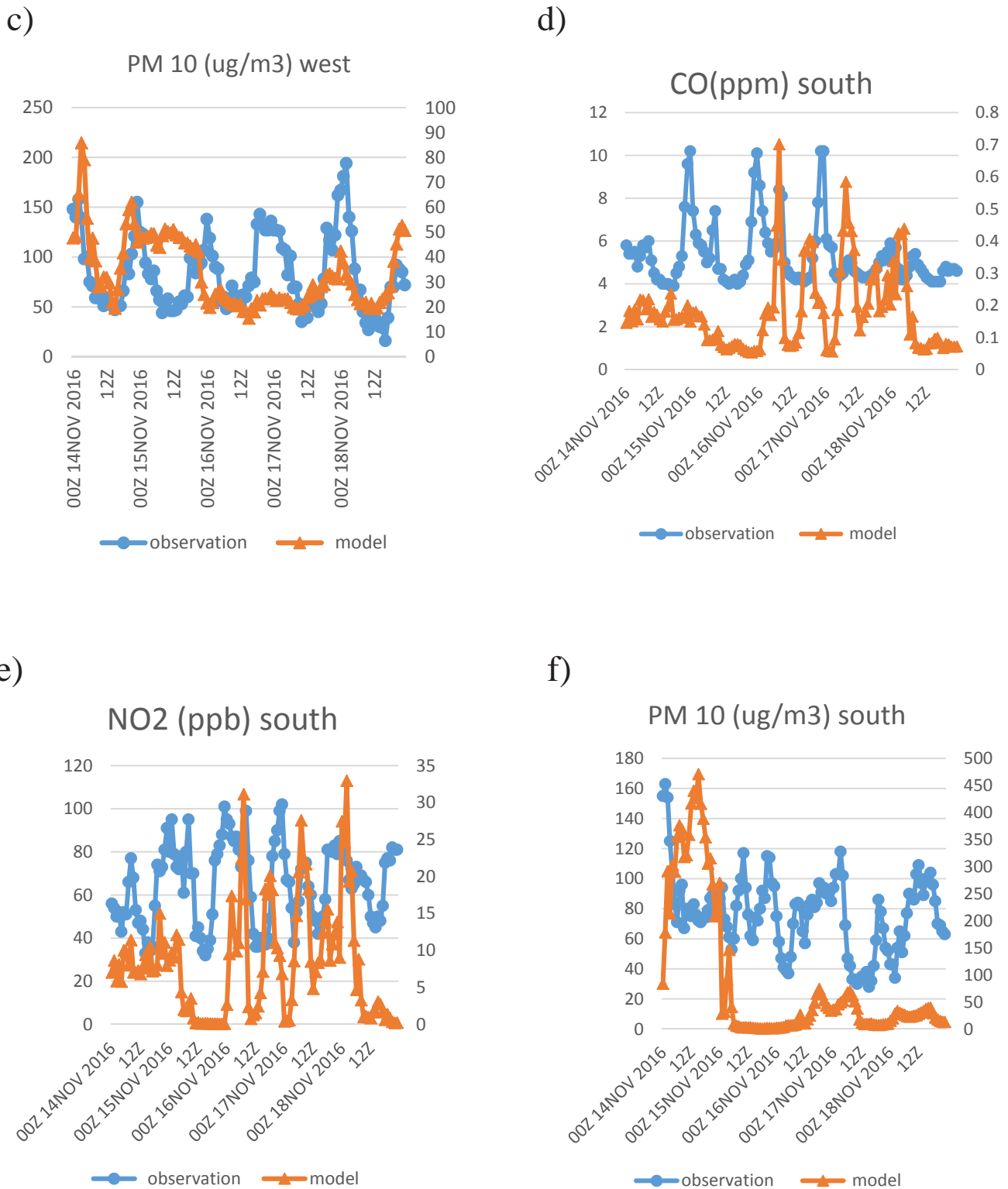
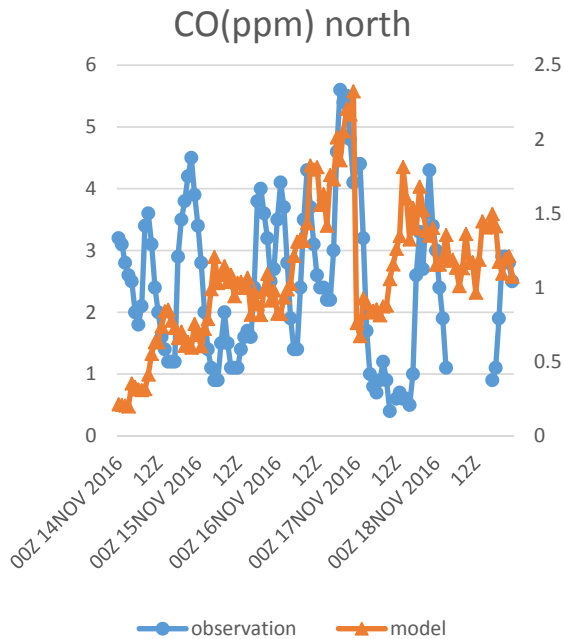
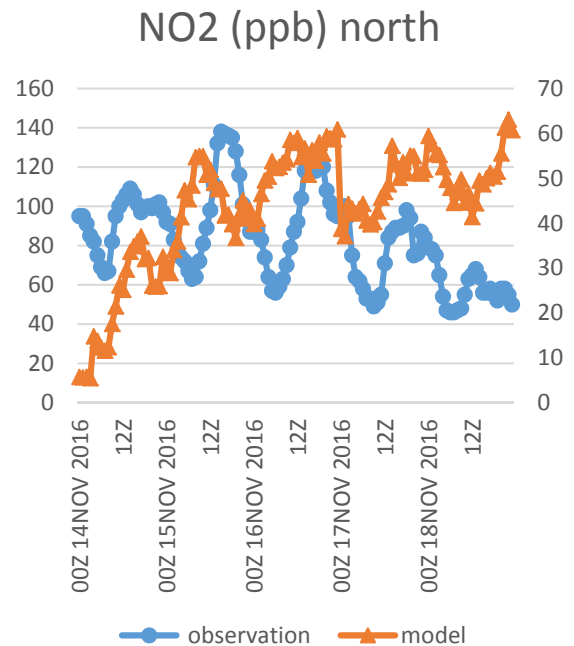


Fig. 14. a, b, and c) Simulated (red diagram, left vertical axis) and observed (blue diagram, right vertical axis) concentrations of CO, NO<sub>2</sub>, and PM<sub>10</sub>, respectively, for the west of Tehran. d, e, and f) same as a, b, and c, for the south of Tehran. g, h, and i) same as a, b, and c, for the north of Tehran

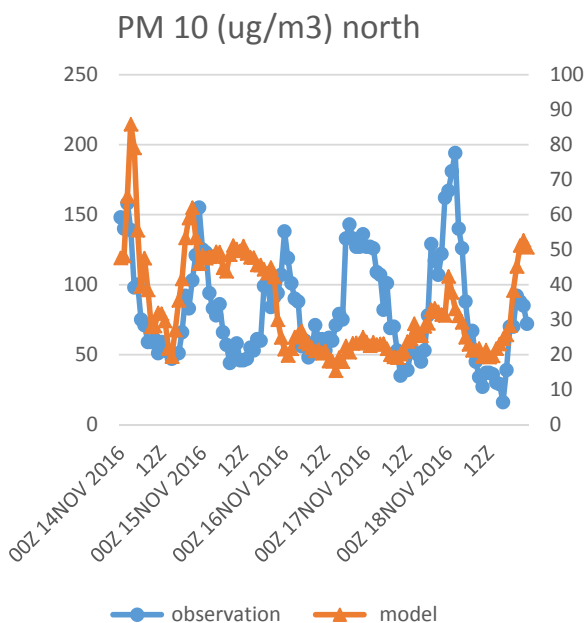
g)



h)



i)



### FINANCIAL SUPPORTS

This study was supported by the Atmospheric Science and Meteorological Research Center.

### COMPETING INTERESTS

The authors have no competing interests.

### ACKNOWLEDGEMENTS

Special thanks to the Iranian Meteorological Organization and Tehran Air Quality Control company for the valuable data used in this study.

### ETHICAL CONSIDERATIONS

The authors state that ethical considerations are fully respected in this study.

### REFERENCES

- [1] Bidokhti AA, Shariepour Z, Sehatkashani S. Some resilient aspects of urban areas to air pollution and climate change, case study: Tehran, Iran. *Scientia Iranica Transaction A, Civil Engineering*. 2016;23(6):1994.
- [2] Brook RD, Franklin B, Cascio W, Hong Y, Howard G, Lipsett M, et al. Air pollution and cardiovascular

Fig. 14. a, b, and c) Simulated (red diagram, left vertical axis) and observed (blue diagram, right vertical axis) concentrations of CO, NO<sub>2</sub>, and PM<sub>10</sub>, respectively, for the west of Tehran. d, e, and f) same as a, b, and c, for the south of Tehran. g, h, and i) same as a, b, and c, for the north of Tehran

- disease: a statement for healthcare professionals from the Expert Panel on Population and Prevention Science of the American Heart Association. *Circulation*. 2004;109(21):2655-71.
- [3] Ruckerl R, Ibalid-Mulli A, Koenig W, Schneider A, Woelke G, Cyrys J, et al. Air pollution and markers of inflammation and coagulation in patients with coronary heart disease. *American journal of respiratory and critical care medicine*. 2006;173(4):432-41.
- [4] O'Neill MS, Veves A, Sarnat JA, Zanobetti A, Gold DR, Economides PA, et al. Air pollution and inflammation in type 2 diabetes: a mechanism for susceptibility. *Occupational and environmental medicine*. 2007;64(6):373-9.
- [5] Mills NL, Donaldson K, Hadoke PW, Boon NA, MacNee W, Cassee FR, et al. Adverse cardiovascular effects of air pollution. *Nature Reviews. Cardiology*. 2009;6(1):36.
- [6] Samet JM, Speizer FE, Bishop Y, Spengler JD, Ferris Jr BG. The relationship between air pollution and emergency room visits in an industrial community. *Journal of the Air Pollution Control Association*. 1981;31(3):236-40.
- [7] Peters A, Dockery DW, Muller JE, Mittleman MA. Increased particulate air pollution and the triggering of myocardial infarction. *Circulation*. 2001;103(23):2810-5.
- [8] Hosseinpour AR, Forouzanfar MH, Yunesian M, Asghari F, Naieni KH, Farhood D. Air pollution and hospitalization due to angina pectoris in Tehran, Iran: a time-series study. *Environmental Research*. 2005;99(1):126-31.
- [9] Kermani M, Dowlati M, Jonidi Jafari A, Rezaei Kalantari R, Sadat Sakhaei F. Effect of air pollution on the emergency admissions of cardiovascular and respiratory patients, using the air quality model: A study in Tehran, 2005-2014. *Health in Emergencies and Disasters Quarterly*. 2016;1(3):137-46.
- [10] Peng RD, Chang HH, Bell ML, McDermott A, Zeger SL, Samet JM, et al. Coarse particulate matter air pollution and hospital admissions for cardiovascular and respiratory diseases among Medicare patients. *Jama*. 2008;299(18):2172-9.
- [11] Dadbakhsh M, Khanjani N, Bahrampour A. Death from respiratory diseases and air pollutants in Shiraz, Iran (2006-2012). *Journal of Environment Pollution and Human Health*. 2015;1(3):4-11.
- [12] Samet JM, Dominici F, Curriero FC, Coursac I and Zeger SL. Fine particulate air pollution and mortality in 20 US cities, 1987-1994. *New England journal of medicine*. 2000;343(24):1742-1749.
- [13] ALIAKBARI BA, SHAREIPOUR Z. Upper air meteorological conditions of acute air pollution episodes (case study: Tehran). 2010.
- [14] Dayan U, Levy I. Relationship between synoptic-scale atmospheric circulation and ozone concentrations over Israel. *Journal of Geophysical Research: Atmospheres*. 2002;107(D24).
- [15] Levy I, Mahrer Y, Dayan U. Coastal and synoptic recirculation affecting air pollutants dispersion: a numerical study. *Atmospheric Environment*. 2009;43(12):1991-9.
- [16] Kallos G, Kassomenos P, Pielke RA. Synoptic and mesoscale weather conditions during air pollution episodes in Athens, Greece. *Transport and Diffusion in Turbulent Fields*: Springer; 1993 .p. 163-84.
- [17] Halek F, Kianpour-Rad M, Kavousirahim A. Seasonal variation in ambient PM mass and number concentrations (case study: Tehran, Iran). *Environmental monitoring and assessment*. 2010;169(1-4):501-7.
- [18] Cimorelli AJ, Perry SG, Venkatram A, Weil JC, Paine RJ, Wilson RB, et al. AERMOD: A dispersion model for industrial source applications. Part I: General model formulation and boundary layer characterization. *Journal of applied meteorology*. 2005;44(5):682-93.
- [19] Scire JS, Strimaitis DG, Yamartino RJ. A user's guide for the CALPUFF dispersion model. Earth Tech, Inc. Concord, MA. 2000;10.
- [20] Stein AF, Draxler RR, Rolph GD, Stunder BJ, Cohen MD and Ngan F. NOAA's HYSPLIT atmospheric transport and dispersion modeling system. *Bulletin of the American Meteorological Society*. 2015; 96(12): 2059-2077.
- [21] Carruthers DJ, Holroyd RJ, Hunt JC, Weng WS, Robins AG, Apsley D, et al. UK-ADMS: A new approach to modelling dispersion in the earth's atmospheric boundary layer. *Journal of wind engineering and industrial aerodynamics*. 1994; 52:139-53.
- [22] Janicke U. Dispersion model LASAT. Reference Book for Version 2.12. Janicke Consulting; 2003.
- [23] Safavi Y, Alijani B. Geographical agents analyzing in air pollution in Tehran. *Geographical Research*. 2006;58(1):106-151.
- [24] Mlawer EJ, Taubman SJ, Brown PD, Iacono MJ, Clough SA. Radiative transfer for inhomogeneous atmospheres: RRTM, a validated correlated-k model for the longwave. *Journal of Geophysical Research: Atmospheres*. 1997;102(D14):16663-82.
- [25] Chou MD, Suarez MJ. An efficient thermal infrared radiation parameterization for use in general circulation models: Citeseer; 1994.
- [26] Noh Y, Cheon WG, Hong SY, Raasch S. Improvement of the K-profile model for the planetary boundary layer based on large eddy simulation data. *Boundary-layer meteorology*. 2003;107(2):401-27.
- [27] Hu XM, Nielsen-Gammon JW, Zhang F. Evaluation of three planetary boundary layer schemes in the WRF model. *Journal of Applied Meteorology and Climatology*. 2010;49(9):1831-44.
- [28] Hong SY, Noh Y, Dudhia J. A new vertical diffusion package with an explicit treatment of entrainment processes. *Monthly weather review*. 2006;134(9):2318-41.